International Journal of Low-Carbon Technologies Advance Access published May 14, 2014

An innovative wind–solar hybrid street light: development and early testing of a prototype

Renato Ricci[1], Daniele Vitali[1]* and Sergio Montelpare[2]
[1]*Università Politecnica delle Marche, via Brecce Bianche 1, Ancona 60131, Italy;*
[2]*Università degli Studi G. D'Annunzio, V.le Pindaro 42, Pescara 65127, Italy*

Abstract

An innovative renewable hybrid microgeneration unit has been designed to be fully embedded into a dedicated LED street lighting system. The key feature of this new concept is the arrangement of a multiple Savonius vertical axis wind turbine into the structure itself of the post. A photovoltaic panel is integrated to contribute to power generation. The energy is collected by a power conversion equipment along with a storage device which ensures the lighting also during windless nights. The main application of this project is the standalone street lighting, but also a grid connected option is feasible, making the system compatible with microgrid concepts. Different Savonius rotors have been designed and characterized by wind tunnel tests. The adopted cylindrical geometry has shown a maximum power factor of 0.21. A dedicated safety equipment has been designed to prevent turbine over-speed by automatic stop in extreme wind condition. A full-scale prototype of the generator/lighting system has been installed. The experimental data acquisition is currently in progress to analyse on site performance and to allow energy simulations.

Keywords: wind–solar hybrid; microgeneration; VAWT; savonius; street lighting

*Corresponding author:
d.vitali@univpm.it

Received 15 July 2013; accepted 18 March 2014

INTRODUCTION

The test of research in renewable energy microgeneration technology is the lucky combination of efficiency and urban integration. Indeed, the application field with the biggest potential is within cities where the number of small consumers is concentrated. Obviously, in this context, the acceptance of people towards the installation of new power plants becomes essential for the success of projects. Wind and solar energy are free and clean sources, maybe the most promising alternative of fossil fuels power generation. This idea has been leading the energy market in recent years. However, small wind turbines in particular have to face some obstacle related to noise, low and turbulent winds and visual impact. Visual annoyance can first rise from the high rotation speed, typical of small wind generators. Building-mounted wind turbines could be a solution [1, 2] to gain elevation over the urban boundary layer, where the available air stream is stronger. Nevertheless, power level of this type of installations is seriously limited by the structural resistance of existing buildings and the transmission of vibrations. This is why an embedded wind power solution would be preferable. Among fields ready for a coupling between electrical sources and load, there is outdoor lighting. Pole structures carrying on lamps can be suited to allow the installation of renewable energy devices. Such systems, especially powered by photovoltaic (PV) panels and batteries, are currently sold. Their main application is the lighting in remote areas, as stand-alone generation units. There are some commercial products provided with both PV and either vertical (VAWT) or horizontal (HAWT) axis wind turbines technology, such as those in references [3, 4].

HAWTs generally take advantage of a greater power factor as shown in Figure 1. However, in the microgeneration field, their aerodynamic efficiency is penalized by the lack of active control, in particular with respect to the yaw error [5] and the start-up operation. Such issues do not involve micro-VAWTs like Savonius type which get competitive, especially in highly variable wind conditions.

The existing solutions typically use vertical axis, mainly Darrieus type, turbines arranged on the top of traditional poles. Power generation units therefore appear geometrically disjointed from the whole street light. Berdanier *et al.* have presented in [6] the incorporation of a Savonius-type wind turbine, along with a tilted PV panel, into the light housing of a light post prototype. This option too is characterized by only one wind rotor on the top of the pole.

International Journal of Low-Carbon Technologies 2014, 0, 1–10

doi:10.1093/ijlct/ctu016

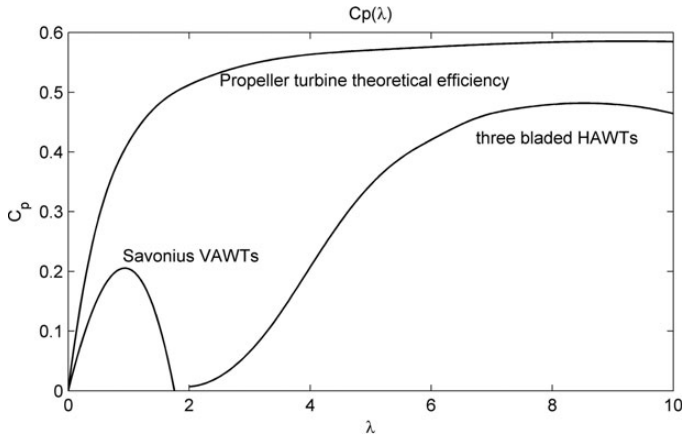

Figure 1. *Typical aerodynamic efficiency C_p: comparison between different wind turbine types.*

The present work has followed the same technological combination concept. The main idea is the full integration of renewable power generation into the same facility which satisfies the electrical energy demand. The result is a new prototype of wind–solar hybrid street lighting system, named *Generator* (Figure 2). The project was aimed to find a feasible compromise between proportionate architecture, energy efficiency and structural effectiveness. It has been developed through a close collaboration between University and industrial partners within a project sponsored by the Italian Ministry of Economic Development. Each partner has contributed to the development in his field of competences:

- wind turbines;
- drive train;
- PV panel;
- LED lamp;
- structure design;
- electronic devices and battery.

A Savonius-type rotor has been studied through wind tunnel tests and designed for the purpose. This type of wind turbine exhibits several advantages with respect to this application, mainly due to its relatively low speed of rotation and its 'vertical' geometry, well incorporated in a slender object such as a street light.

The outdoor lighting represents a crucial source of security given to citizens. In order to preserve this purpose, a special attention has been paid both to the safety systems of wind rotors and to the supervision system with an Information and communications technology interface, which is capable of broadcasting to a server all real-time state variable of the machine.

Generator prototype has been installed at Politechnic University of Marche where it has been giving field experimental data in association to a dedicated 10 m meteorological tower, which allows a full-energy characterization of the hybrid microgeneration system. All experimental information will be used to evaluate the potential behind this concept and to focalize the improvement areas of the system.

Figure 2. 'Generator' *prototype: a rendering and a night photo.*

THE *GENERATOR* PROTOTYPE

This novel hybrid street light is constituted of three main substructures:

- the multi-pile supporting structure provided with the alternator and hardware vanes;
- the multi-pile wind turbines structure, which houses the three Savonius rotors through two bearings each. For the sake of security, they stay well above the pedestrian height, i.e. >3 m above the ground;
- the top lighting and photovoltaic body.

The structural concept has followed an evolution over the time of the *Generator* project, led by economic considerations (Figure 3). The first type was a much more closed construction, due to a load-bearing sheet metal basement and to the presence of adjustable stators around the turbines. Moreover, the top body carrying the PV was bulkier in order to collect more solar energy. With the second generation, the configuration has

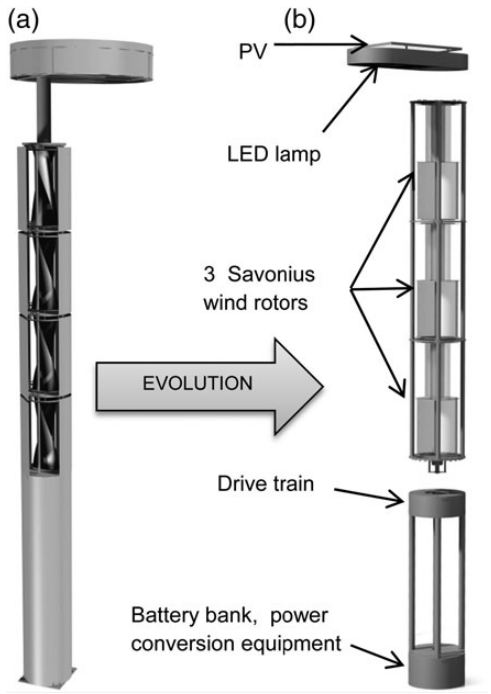

Figure 3. *First (**a**) and second (**b**) generation prototype (CAD). Separation into the main sub-structures.*

turned to a visibly lighter and more slender 9 m high structure, based on four structural steel pipes bonded together by steel plates.

The dimension of the four pillars had to be a compromise between the minimization of aerodynamic interference with turbines and the pole stiffness. Within this frame are arranged three Savonius two-stage VAWTs, which are directly connected each other and rotate jointly into overall six adjustable bearings. Unlike the prime ones, these rotors do not have a central shaft, so their buckets have to be sized to transmit torque. In this respect, the lowest rotor is obviously the most loaded. The mechanical power is transmitted directly to a permanent magnet synchronous generator (PMSG) located within the drive train space, at 3 m of height. The alternator through a three-phase rectifier (AC/DC) and the photovoltaic panel on the top of the lamp-post feed electrical energy to the hybrid power controller in the space at the bottom. Power is then transferred to the DC battery bus, which powers the light-emitting diode (LED)-based lamp, besides the control equipment itself. Moreover, the system is prepared also for grid connection through an inverter devoted to eventual load balancing needs (Figure 4).

The PV panel is approximately horizontal, and its inclination is only some degree for precipitation issues. This choice is principally based on aesthetic reason, within the smooth architecture of the prototype. The null tilt angle can be a problem concerning the energy autonomy of such a system especially in winter and at high latitudes. Lagorse *et al.* [7] suggest to associate the PV source with a fuel cell within a stand-alone street light. In this work, instead, the absent tilt of the panel is expected to be

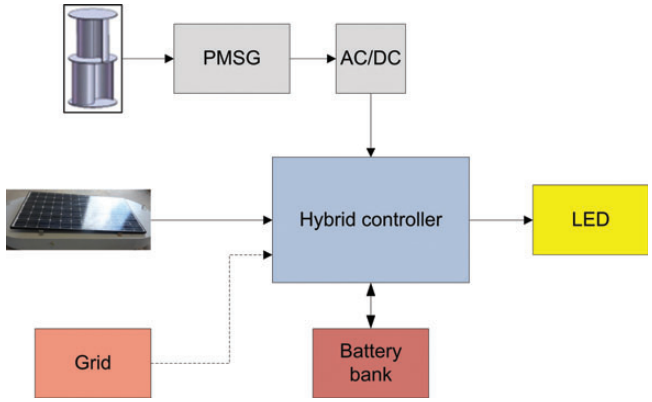

Figure 4. *Diagram of the hybrid system.*

compensated by the energy generation of wind turbines. This way the geometrical concept of Generator is preserved. Moreover, future installations would not need to be adjusted towards the south, keeping the omni-directionality advantage given by VAWTs. The PV module is mounted on the top of the lighting body. It is a 215-W maximum power panel using heterojunction with intrinsic thin layer (HIT) technology. This panel potential efficiency is 17.2%.

In order to achieve the least energy consumption, the street light is provided with LED luminaires technology, which is a promising option for future outdoor lighting. LEDs allow energy savings along with longer lifetimes compared with traditional lighting [8]. The selected product for the project is Philips Rebel Luxeon with an efficiency of 100 lm/W. The lamp hold overall 60 LEDs capable of 6000 lm luminous flux.

Power conversion fit the electrical energy to be thrown into the DC bus at the battery voltage level. A three-phase rectifier and a DC–DC buck converter are used in wind turbine generation. A solar DC–DC converter also adapts the PV voltage for the charging purpose. The whole power conditioning equipment has been developed specifically for *Generator*. Currently, dedicated maximum power point tracking (MPPT) control are being investigated for both renewable energy devices.

The adopted storage devices are lead acid gel deep-cycle batteries, each with 12 V nominal voltage. Four units are connected in series in a bank at 48 V. The battery capacity is currently 40 Ah. The storage sizing was at first aimed at the autonomy of two nights of lighting without available energy sources. However, the actual system effectiveness over time is being evaluated through current field tests.

THE WIND TURBINES

The selected wind turbines for this renewable energy system are Savonius rotors, which take their name from their Finnish inventor (1925). They consist of VAWTs based predominantly on the action of drag aerodynamic force over two buckets with an 'S-shaped' cross section (Figure 5). Indeed, this rotor is a low

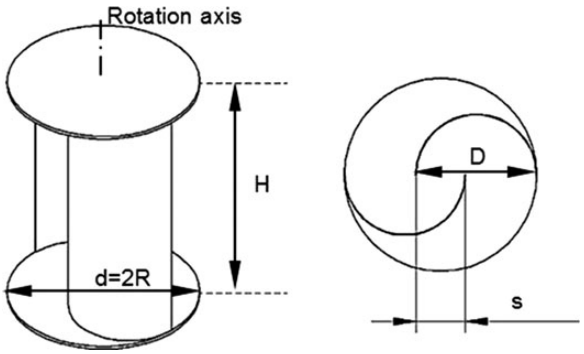

Figure 5. *Cylindrical Savonius with end plates: main geometry parameters.*

lift to drag ratio machine [9]. The principle that makes a Savonius receiving torque and so power from air stream is similar to that of cup anemometers: the wind generates a drag imbalance between the concave advancing bucket and the convex retreating one.

Such VAWTs do not reach a high aerodynamic efficiency compared with standard HAWTs but they exhibit several advantages interesting in small power units [10, 11]:

- simple technology with low cost;
- wind acceptance from any direction, without the need of yawing mechanism;
- low noise and rotation speed;
- reduced wear on moving parts;
- various rotor configuration options;
- high static moment useful for start-up operation.

Various rotor configurations have been defined for this project. Each geometrical parameter has an important effect on VAWT power performances [10] and has been evaluated and verified through wind tunnel tests, at Polytechnic University of Marche, with the experimental procedure explained in [12, 13]. These are the main adopted rotor features:

- semi-circular cross section for simplicity of construction;
- overlap ratio $s/D = 0.23$ compatible to optimum performance criteria [10, 14];
- module aspect ratio $H/d = 1.8/0.7 = 2.57$;
- end plates to rise performances;
- absence of shaft: rotors have a role in transmitting torque to the drive train;
- two-stage rotor (90° staggered each other), in order to smooth aerodynamic static moment and to confer structural stability to the rotor through an intermediate plate.

A key aerodynamic issue of this prototype is the penalizing effect of the multi-pole structure surrounding the VAWTs. This has been evaluated using a mono-stage 1:1.8 scaled Savonius model along with four poles similar to the full*scale structure. The object was delimited from end plates in order to make the flux as 2D as possible. Figure 6 shows the tested configuration having one pillar in front of the wind tunnel air stream.

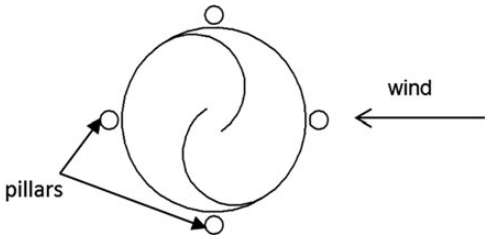

Figure 6. *Scheme of test model section in wind tunnel experiments.*

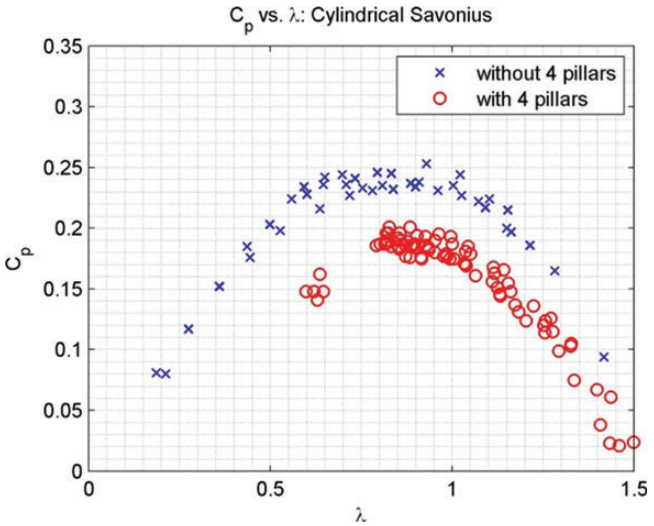

Figure 7. *Experimental power factor of straight Savonius rotor: effect of four external pillars.*

The angular speed ω (rad/s) and the load torque M (Nm) of the model were measured by means of an incremental encoder and a load cell [13]. The investigated wind speed was ranging between 6 and 12 m/s. The measured quantities were arranged into the common adimensional parameters of wind turbines, i.e. the moment coefficient C_m and the power coefficient C_p. Both were evaluated as function of tip speed ratio λ.

$$C_m = \frac{M}{\frac{1}{2}\rho u_\infty^2 RA} \quad (1)$$

$$C_p = \frac{P}{\frac{1}{2}\rho u_\infty^3 A} \quad (2)$$

$$\lambda = \frac{\omega R}{u_\infty} \quad (3)$$

where $A = 2R{\cdot}H$ is the frontal area of a rotor, R is the radius, H is the height, u_∞ is the incoming wind speed and ρ is the air density.

As illustrated in Figure 7, maximum power coefficient C_p undergoes a visible decrement because of poles interference (from 0.24 to 0.18).

Another rotor configuration developed within this study is a helical Savonius, with a 105° maximum section rotation. Its wind tunnel model without pillars demonstrated a maximum power factor very close to the straight model, next to 0.25 (Figure 8).

The most remarkable result is the better performance of helical rotor with the presence of pillars. C_p values reach the maximum of 0.21 and, moreover, they keep at a higher level also at greater tip speed ratios. This turns to be the most desirable configuration for *Generator* and is one of the reasons that suggested the option of two-stage straight rotors, what represents a discretized-like helical feature, with simpler construction. The power advantage of helical with four pillar (105deg4P) is more evident from the polynomial regression of $C_p(\lambda)$ in Figure 9.

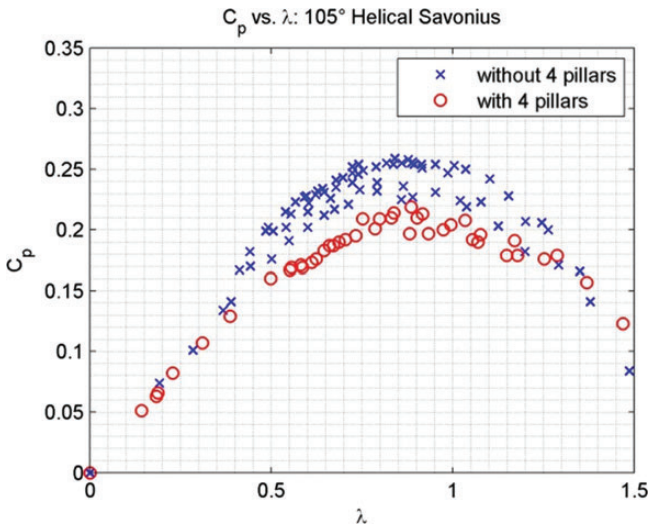

Figure 8. *Experimental power factor of helical Savonius rotor: effect of four external pillars.*

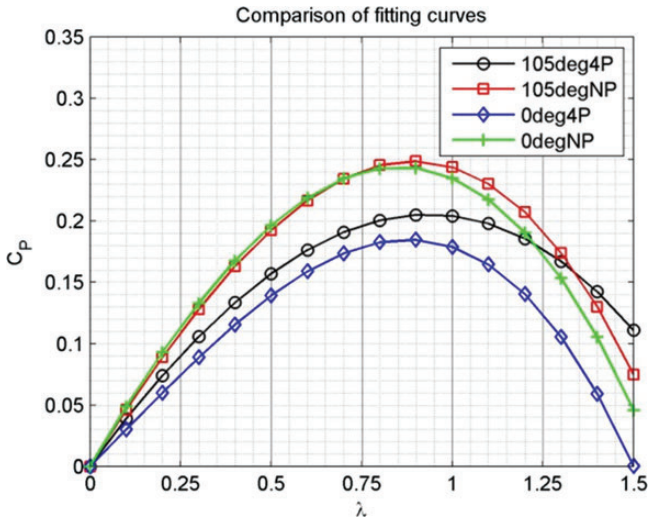

Figure 9. *Third-order polynomial fitting with zero intercept of wind tunnel experimental power coefficient curves.*

The helical rotor performance within the pillar structure can be calculated through the following fitting polynomial.

$$C_p = -0.04078\lambda^3 - 0.1587\lambda^2 + 0.4039\lambda \qquad (4)$$

The variable speed operation of wind turbines consists of tracking (MPPT) the optimal tip speed ratio ($\lambda_{opt} = 0.94$ for the case) through the generator torque controller. This makes the turbine deliver the maximum power at every wind speed.

However, a maximum rounds per minute (RPM) condition imposes a deviation from optimal curve. In order to harness wind energy at higher speed, it would be advantageous to track mechanical power equilibrium along the vertical segment at fixed rotation (Figure 10).

The two-stage straight Savonius rotor has been made of transparent poly-methyl-methacrylate (PMMA), which gains an aesthetical value besides an acceptable strength. The helical version has been realized in fiber-glass-reinforced polyester. The more complex geometry required the construction of dedicated moulds (Figure 11). This composite material guarantees a bigger strength with respect to both static and dynamical loads. One key design parameter of the wind generator is the maximum rotation speed allowed by materials. PMMA rotor provided with 6-mm-thick buckets has shown in finite element method analysis a critical centrifugal stress state at about 290 rpm. In order to stay well apart from this state, the current maximum rotational speed is set to 250 rpm. The controller should activate the brake to avoid over-speed. Such a limit influences the efficiency at high wind speed. Its effect can be evaluated through a simple estimate applying Weibull wind statistics. The wind turbine mean power versus the system maximum RPM is shown in Figure 12. Due to infrequence of high wind speeds, it makes no sense to overcome 200/250 RPM.

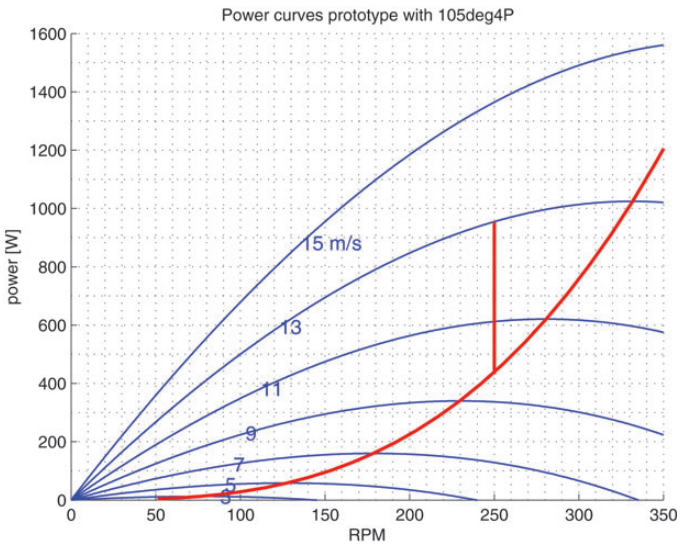

Figure 10. *Aerodynamic power curves of 105deg4P. Parabolic and vertical lines represent ideal power with or without RPM limit.*

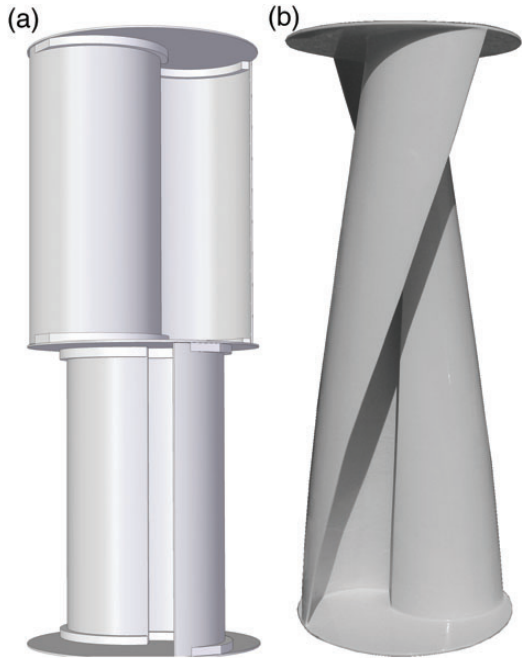

Figure 11. *Constructed prototypes of Savonius rotors: (**a**) two-stage straight and (**b**) helical configurations.*

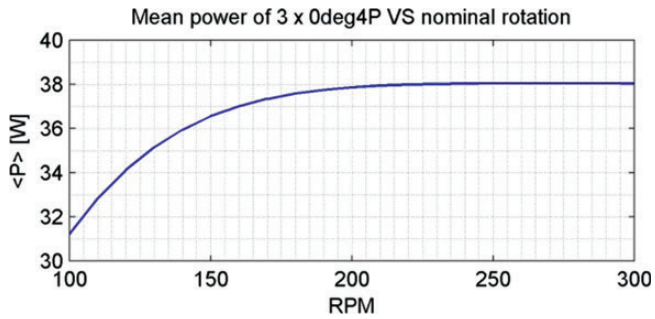

Figure 12. *Weibull method expected mean power from three straight Savonius as a function of their maximum RPM.* (k = *1.98;* c = *4.18).*

The whole Savonius train is directly coupled through a joint to a three-phase PMSG. Its main characteristics are:

- rated speed: 350 rpm;
- rated power: 1444 W;
- voltage at rated power: 232 V;
- polar pairs: 12;
- efficiency at rated power: 75%.

The system is equipped with both a mechanical brake and an electromagnetic brake, using dump loads connected to alternator electrical output.

As wind speed and RPM rise over the cut-out limits, which for instance are currently fixed at 250 rpm and 14 m/s, the controller automatically switch the DC load from the battery to the dump load, making the alternator a viscous-like brake. This operation is used to slow the rotors. Then a disc brake is operated in order to bring turbines to rest. A Savonius VAWT is indeed a more insecure machine than classical HAWTs at extreme wind conditions, because of the absence of stall phenomena.

The mechanical brake system has been designed to keep rotors at rest also without actuator powering. This is made possible by an irreversible mechanism that pushes brake pads against the brake disc.

ON-SITE TESTING AND EVALUATION

Field experimentation

The prototype has been installed at Engineering Faculty in Ancona in order to test its performance over different possible configurations. *Generator* measurement system samples all experimental data with a time rate of about 6 s. A signal conditioning unit interfaces to the power electronics through several transducers such as Hall effect ammeters. Real-time data are then transmitted by GPRS to a dedicated server. The following physical variables are being acquired:

- battery voltage
- PV voltage
- Solar DC bus current
- Wind rectifier voltage
- Wind DC bus current
- Wind generator RPM
- Load DC-bus current
- Wind speed

The local wind speed is measured by a little cup anemometer on the top of the lamp-post, while the rotation speed is evaluated by means of an inductive proximity sensor.

Moreover, the full characterization of this renewable energy microgeneration system is made possible by a 10-m high meteorological tower which is about 100 m distant southward with respect to the prototype and about 10 m above it. The location is on Monte D'Ago hill and the top anemometer is at 172 m above sea level. The apparatus, for the purpose in particular, is equipped with:

- Cup anemometer;
- Wind vane gonioanemometer;
- Global radiation sensor (over horizontal surface);
- Direct radiation sensor;
- Thermometer.

The met tower makes use of a global system for mobile communications, to allow periodically the download. The measured weather data are aggregated through mean, maximum and minimum over 10 min intervals.

The installation site has been characterized, from a wind energy point of view, by a 1 year (from 5 October 2011 to 5 October 2012) weather data collection with the met tower

anemometer. The best-fit Weibull distribution is shown in Figure 13 and its resulting parameter values are $k = 1.98$ and $c = 4.18$. The mean wind speed over the year is 3.7 m/s. This value is not actually appropriate for a traditional wind farm, so it is important to choose a micro wind technology with good efficiency at low wind speed, as in typical urban areas.

The site frequency rose is shown in Figure 14 and it indicates two prevailing directions (S and NNW).

Indeed, these directions are associated with the local sea breezes.

In order to conveniently correlate the met tower wind measurements with the wind energy production at the *Generator* site, the wind speed-up factors between the two sites have been calculated. The wind speed data from lamp-post anemometer u_{Gen} were averaged at the same sample time of tower data u_{tower}.

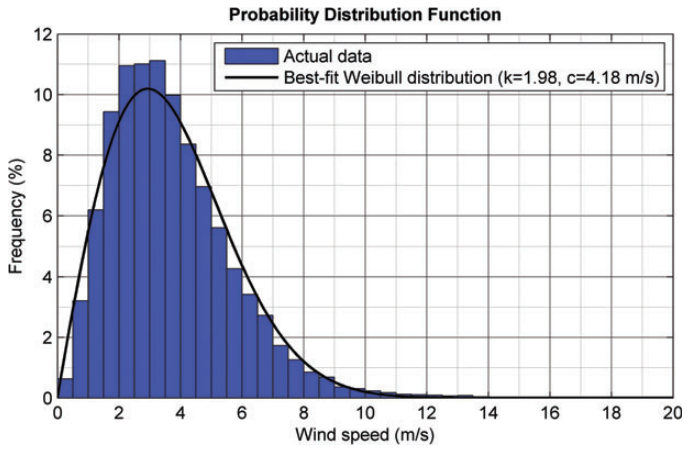

Figure 13. *Wind speed Weibull distribution relative to the installation site. $k = 1.98$; $c = 4.18$ (generated using Windographer).*

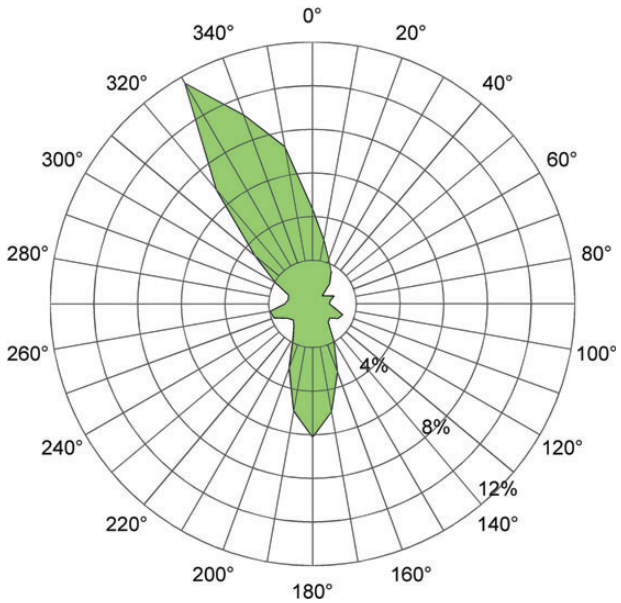

Figure 14. *Wind frequency rose of Monte D'Ago hill met tower (generated using Windographer).*

In relation to the direction of air stream at the tower, the ratio $u_{\text{Gen}}/u_{\text{tower}}$ produces the polar scatter plot in Figure 15.

The speed-up points are fitted using a harmonic regression with up to five frequencies:

$$v(\theta) = c + \sum_{j=1}^{5} a_k \sin\left(\frac{2\pi j\theta}{360}\right) + b_j \cos\left(\frac{2\pi j\theta}{360}\right) \qquad (5)$$

The resulting polar curve highlights a remarkable wind speed reduction on the street-light system with wind velocities coming

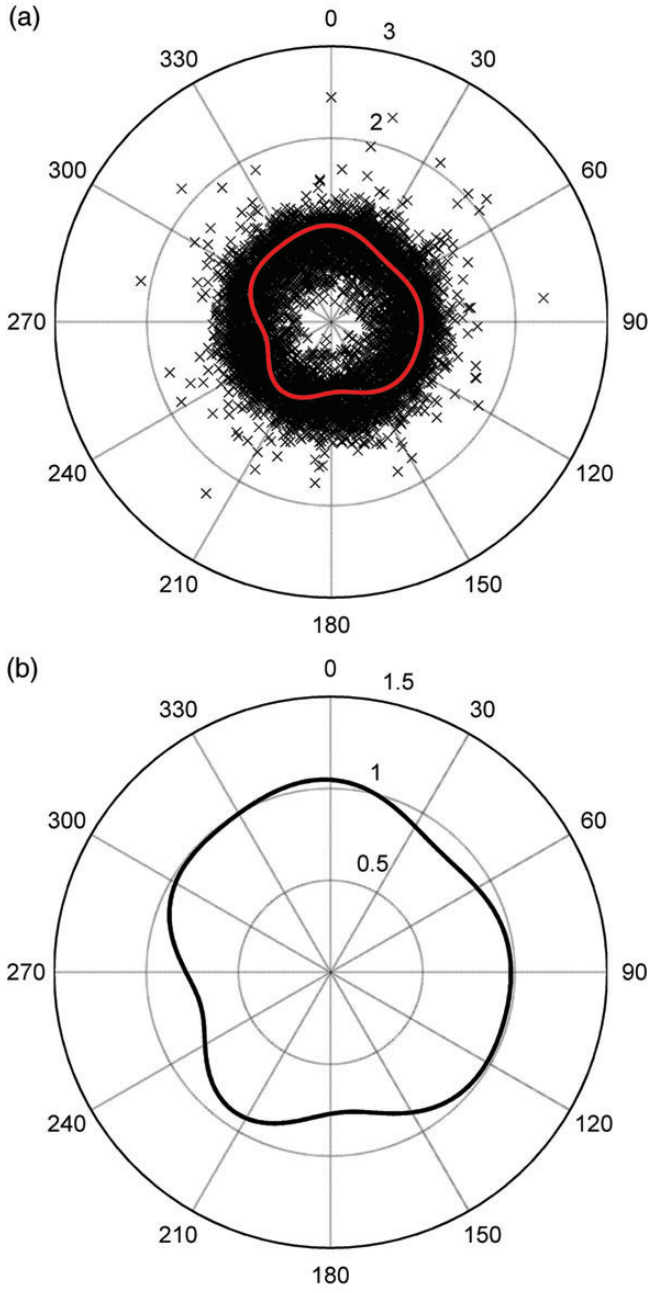

Figure 15. *Polar scatter plot of speed-up factor over wind direction and harmonic regression.*

from west and south. This is consistent with the local orography and obstacles: southward the hill itself while westward a forest act as a wind shadow. In all other cases, the speed levels appear quite similar at both locations.

Prototype early testing

The early test results are collected here. A MATLAB program has been written for importing and processing experimental data. The global and direct radiation measured by tower sensors in two specific days are shown in Figure 16.

The LED consumption has been derived from voltage and current measures.

$$\begin{aligned} P_{\text{load}} &= V_{\text{batt}} I_{\text{load}} \\ P_{\text{LED}} &= P_{\text{load}} - P_{\text{auxiliary}} \end{aligned} \tag{6}$$

The state of lighting is inferred using a power load threshold of 35 W. Indeed, when LED lamp is turned off, auxiliary load associated with power and signal conditioning devices is about 10 W, well below the threshold. LED system consumption instead has showed a mean value of 78 W.

It should be noticed that there is a quite precise correspondence between twilight switching and the zero-value global radiation.

Making use of the available global radiation measure over horizontal surface, it is immediate to calculate the available solar energy incident and then the operating electrical efficiency of PV panel on the top of light post. The power delivered by PV and the available power are here obtained:

$$\begin{aligned} P_{\text{PV}} &= V_{\text{batt}} I_{\text{PV-dc}} \\ P_{\text{available}} &= R_{\text{glob}} \cdot A_{\text{PV}} \end{aligned} \tag{7}$$

where $A_{\text{PV}} = 1.2$ m^2 is the panel surface. The PV does not generate power when global radiation R_{glob} is <200 W/m^2. The resulting scatter plot along with a parabolic regression of PV efficiency is present in Figure 17.

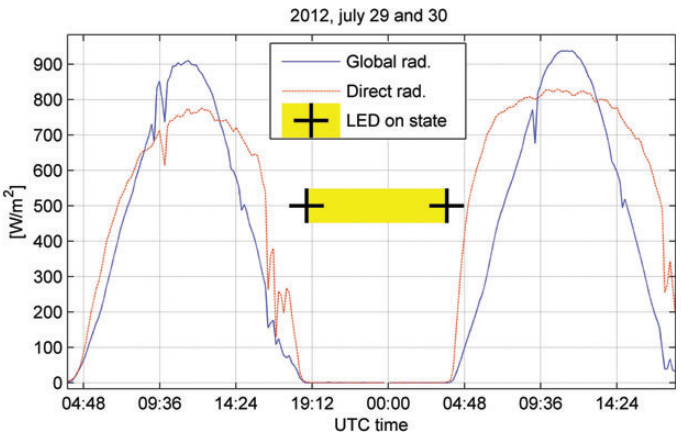

Figure 16. *LED lighting in night hours.*

The mean experimental efficiency is 10.7%, calculated as energy generated over interval T divided by incident radiation.

$$\eta_{\text{PV,tot}} = \frac{\int_{\text{T}} P_{\text{PV}} dt}{\int_{\text{T}} R_{\text{glob}} \cdot A_{\text{PV}} dt} \tag{8}$$

The PV generator will reach higher efficiency level after the ongoing power electronic improvement.

Finally, it is explored the free rotation behaviour of wind turbine. The *Generator* has been tested without generating electrical power, with the alternator electrically disconnected from load. In Figure 18 is shown the rotation speed in relation to the corresponding wind speed from prototype anemometer. For every value of instantaneous wind speed, all values of RPM below a certain level are present. This is explained through transient dynamics of the rotor train subjected to a very variable aerodynamic torque, as a consequence of the intrinsically fluctuating nature of wind, especially in presence of diffused obstacles

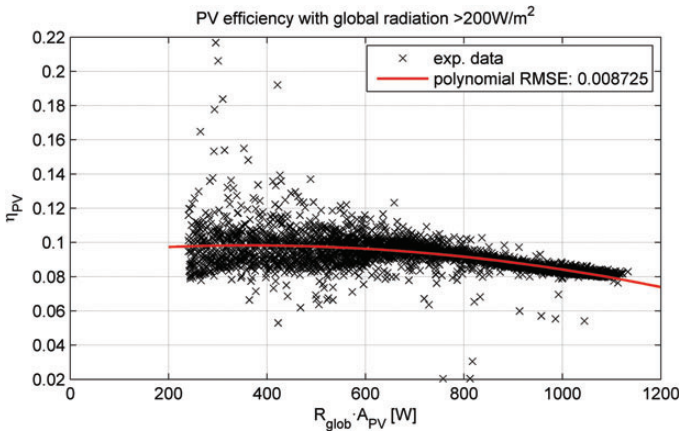

Figure 17. *PV generator efficiency.*

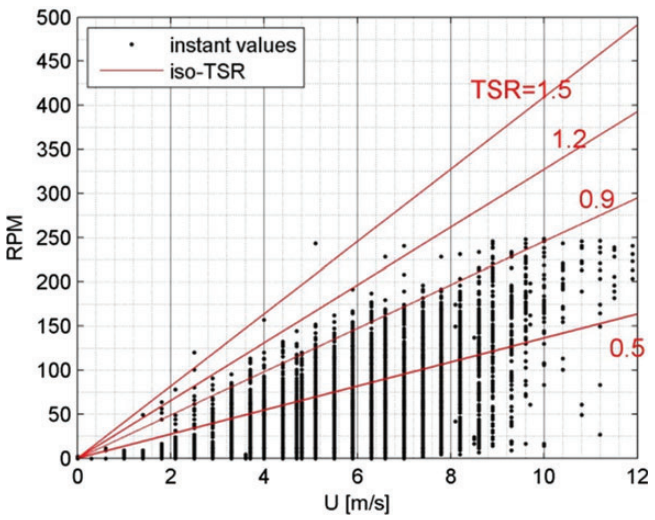

Figure 18. *Wind turbine RPM versus wind speed from prototype anemometer.*

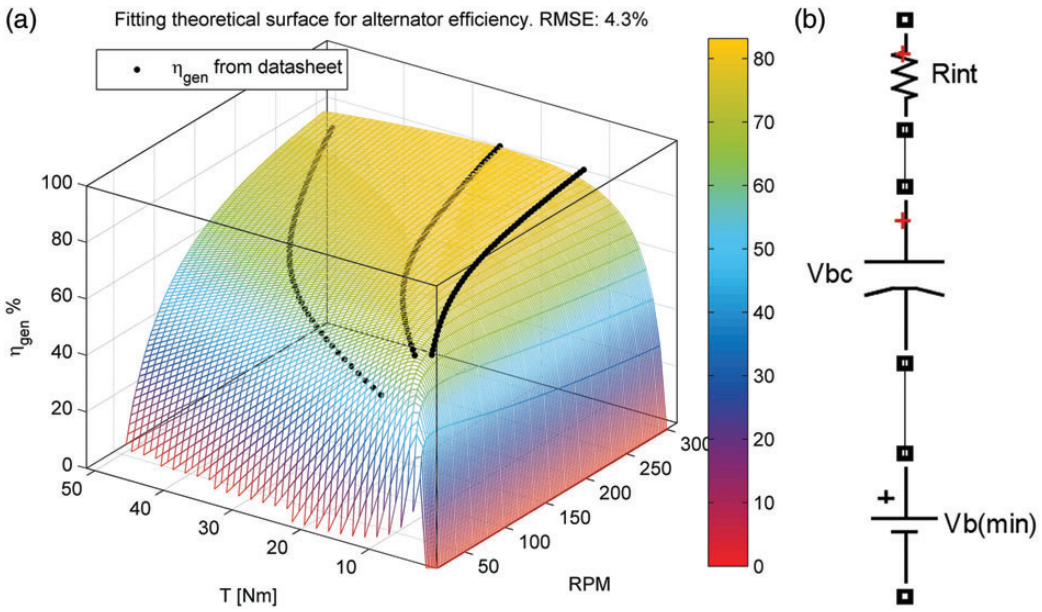

Figure 19. *(**a**) Alternator efficiency surface. (**b**) Electrical model of battery.*

like in this case. The superior bound of the scatter graph approximately coincides with the $\lambda = 1.2$ straight line. The expected free rotor tip speed ratio would be around 1.5, according to Figure 9. This experimental reduction is due to the bigger turbulence with respect to wind tunnel test, besides the mechanical friction losses. The maximum rotation level of 250 rpm is guaranteed from the mechanical brake.

Energy model

The purpose of this simple energy model is to predict the energy performance of the hybrid prototype, in particular its capability to meet the load power requirements. The implemented model calculates the evolution of the physical state of the machine according to the experimental performance curves derived so far and the available meteorological data. The main parameters that describe the effectiveness of the system are the autonomy, in terms of the energy saving from conventional power generation and the lighting reliability.

The method is based upon the local met tower data of solar radiation and wind velocity, corrected by speed-up factors. It makes use of ideal power curve shown in Figure 10 for the wind turbine production and of the efficiency in Figure 17 for the photovoltaic production. The alternator is modelled using an efficiency surface $\eta(RPM,M)$ fitting analytically the manufacturer curves (Figure 19a).

The lead acid deep-cycle battery installed in the hybrid device is modelled through a capacitor, a voltage source and an internal resistance (Figure 19b), besides the coulombic efficiency applied to capacitor, as proposed in reference [15]. Then, the electrical loads are taken into account i.e. the LED lamp and the electronic devices consumption. The hybrid controller is implemented as a set of logical conditions mostly related to:

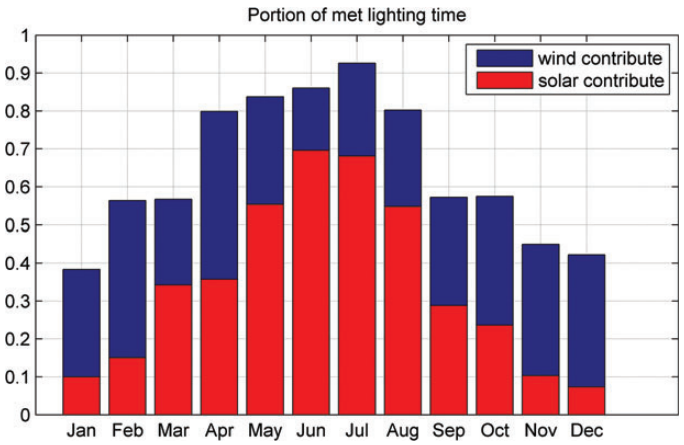

Figure 20. *Lighting reliability over the simulated year. Comparison between energy sources contributions.*

- High-wind condition causing the machine cut-out.
- Low-wind condition: below cut-in speed.
- Low-battery condition: all loads are disconnected.
- Full-charge condition: renewable energy sources are switched off.

The 1-year simulations point out that the current prototype in stand-alone configuration, as modelled here, would meet 61% of hours with lighting need. The low battery state would limit the working time. In Figure 20, there are the contributions of wind and solar sources to the lighting task of the hybrid system over the simulated year. Although the low mean wind speed (3.7 m/s), the wind generator plays a fundamental role in winter as expected, when the solar energy on the horizontal panel falls drastically at medium/high latitudes.

The model indicates also the sensitivity of the energy saving with respect to the possible system improvements. With a PV generator global efficiency up to 15%, the met lighting time would be nearly 73%.

CONCLUSION

The prototype resulting from this project consists of one of the very first wind–solar energy street-lighting systems. The main innovative feature is the full integration of VAWT Savonius rotor along the structure of the lamp-post. This solution allows the exploitation of a considerable wind rotor frontal area and then has a wide potential of productivity, eventually also with grid exchanging. Two Savonius rotor options have been designed and realized according to wind tunnel tests geometrical optimization and to the most appropriate nominal speed of rotation for security and efficiency. A safety brake system has been designed and successfully tested during free rotor operation.

It has been set-up a field test for the wind and solar energy microgeneration unit, based on a meteorological tower and a dedicated algorithm for the correlation of wind speed measurements.

Such a detailed experimental apparatus is devoted to give the tools for a comprehensive study of the renewable energy system. Besides, the performance evaluation of wind–solar devices, experimentation allows to test different control strategies e.g. related to LED switching/dimming and rotor braking criteria.

Further work is being done about the dedicated hybrid power control of Savonius and PV, in order to optimize the MPPT. Such electronic optimization has the purpose to push the self-sustainability of the system towards lower wind speeds.

Moreover, on-site data are currently being used to validate the energy simulation model for an accurate performance prediction at various latitudes and wind conditions.

ACKNOWLEDGEMENT

This project was funded by the Italian Ministry of Economic Development within 'Industria 2015', Bando Innovazione Industriale 'Efficienza Energetica', codice domanda EE01_00054, progetto 'Generator'.

REFERENCES

[1] Dayan E. Wind energy in buildings. *Refocus* 2006;**7**:33–8.
[2] Chong WT, Fazlizan A, Poh SC, *et al*. Early development of an innovative building integrated wind, solar and rain water harvester for urban high rise application. *Energy Build* 2012;**47**:201–7.
[3] Windela. Wind and solar streetlights. http://www.windela.fr/ (18 April 2014, date last accessed).
[4] Urban Green Energy. Wind solar hybrid streetlights. http://www.urbangreenenergy.com/solutions/wind-solar-hybrid-streetlights (18 April 2014, date last accessed).
[5] Rogers T, Omer S. Yaw analysis of a micro-scale horizontal-axis wind turbine operating in turbulent wind conditions. *Int J Low-Carbon Technol* 2012;**8**:58–63.
[6] Berdanier RA, Hernandez KE, Raye CP, *et al*. Integrating Vertical-Axis Wind Turbines and Photovoltaic Solar Cells to Power a Self-sustaining Outdoor Light Source. In: *7th International Conference on Indoor Air Quality, Ventilation and Energy Conservation in Buildings*. Syracuse University, USA, 2010.
[7] Lagorse J, Paire D, Miraoui A. Sizing optimization of a stand-alone street lighting system powered by a hybrid system using fuel cell, PV and battery. *Renew Energy* 2009;**34**:683–91.
[8] Sperber AN, Elmore AC, Crow ML, *et al*. Performance evaluation of energy efficient lighting associated with renewable energy applications. *Renew Energy* 2012;**44**:423–30.
[9] Paraschivoiu I. State of the art of vertical axis wind turbines. In: *Wind turbine design with emphasis on Darrieus concept*, , 2002. pp. 15–36. .
[10] Akwa JV, Vielmo HA, Petry AP. A review on the performance of Savonius wind turbines. *Renew Sustain Energy Rev* 2012;**16**:3054–64.
[11] Fernando MSUK, Modi VJ. A numerical analysis of the unsteady flow past a Savonius wind turbine. *J Wind Eng Ind Aerodyn* 1989;**32**:303–27.
[12] Ricci R, Montelpare S, Borrelli G, *et al*. Experimental analysis of a Savonius wind rotor for streetlighting systems. In: *ASME-ATI-UIT Conference on Thermal and Environmental Issues in Energy Systems*. Sorrento, Italy, 2010.
[13] D'Alessandro V, Montelpare S, Ricci R, *et al*. Unsteady aerodynamics of a Savonius wind rotor: a new computational approach for the simulation of energy performance. *Energy* 2010;**35**:3349–63.
[14] Fujisawa N. On the torque mechanism of Savonius rotors. *J Wind Eng Ind Aerodyn* 1992;**40**:277–92.
[15] Borowy BS, Salameh ZM. Dynamic response of a stand-alone wind energy conversion system with battery energy storage to a wind gust. *IEEE Trans Energy Convers* 1997;**12**:73–8.